Arabidopsis thaliana ggt1 photorespiratory mutants maintain leaf carbon/nitrogen balance by reducing RuBisCO content and plant growth

Younes Dellero, Marlène Lamothe Sibold, Mathieu Jossier, Michael Hodges

the plant journal

SEB Society for Experimental Biology

The Plant Journal (2015) **83**, 1005–1018 doi: 10.1111/tpj.12945

Arabidopsis thaliana ggt1 photorespiratory mutants maintain leaf carbon/nitrogen balance by reducing RuBisCO content and plant growth

Younès Dellero, Marlène Lamothe-Sibold, Mathieu Jossier and Michael Hodges*

Institute of Plant Sciences Paris-Saclay, UMR 9213/UMR1403, CNRS/INRA, Université Paris Sud, Université d'Evry, Université Paris-Diderot, Bâtiment 630, Orsay Cedex 91405, France

Received 16 April 2015; accepted 20 July 2015; published online 28 July 2015.
*For correspondence (e-mail michael.hodges@u-psud.fr).

SUMMARY

Metabolic and physiological analyses of glutamate:glyoxylate aminotransferase 1 (GGT1) mutants were performed at the global leaf scale to elucidate the mechanisms involved in their photorespiratory growth phenotype. Air-grown *ggt1* mutants showed retarded growth and development, that was not observed at high CO_2 (3000 μL L^{-1}). When compared to wild-type (WT) plants, air-grown *ggt1* plants exhibited glyoxylate accumulation, global changes in amino acid amounts including a decrease in serine content, lower organic acid levels, and modified ATP/ADP and $NADP^+$/NADPH ratios. When compared to WT plants, their net CO_2 assimilation rates (A_n) were 50% lower and this mirrored decreases in ribulose-1,5-bisphosphate carboxylase/oxygenase (RuBisCO) contents. High CO_2-grown *ggt1* plants transferred to air revealed a rapid decrease of A_n and photosynthetic electron transfer rate while maintaining a high energetic state. Short-term (a night period and 4 h of light) transferred *ggt1* leaves accumulated glyoxylate and exhibited low serine contents, while other amino acid levels were not modified. RuBisCO content, activity and activation state were not altered after a short-term transfer while the ATP/ADP ratio was lowered in *ggt1* rosettes. However, plant growth and RuBisCO levels were both reduced in *ggt1* leaves after a long-term (12 days) acclimation to air from high CO_2 when compared to WT plants. The data are discussed with respect to a reduced photorespiratory carbon recycling in the mutants. It is proposed that the low A_n limits nitrogen-assimilation, this decreases leaf RuBisCO content until plants attain a new homeostatic state that maintains a constant C/N balance and leads to smaller, slower growing plants.

Keywords: *Arabidopsis thaliana*, photorespiration, photosynthesis, primary metabolism, ribulose-1,5-bisphosphate carboxylase/oxygenase, serine.

INTRODUCTION

Plants fix atmospheric CO_2 and O_2 to produce either 3-phosphoglycerate (3-PGA) or 2-phosphoglycolate (2-PG) by the activity of their ribulose-1,5-bisphosphate (RuBP) carboxylase/oxygenase (RuBisCO). 3-PGA is used directly by plants as a carbon source for biosynthetic processes, including the regeneration of RuBP by the Calvin cycle. Since 2-PG can inhibit the activity of triose phosphate isomerase (necessary for the functioning of the Calvin cycle) (Anderson, 1971), it is metabolized by the photorespiratory cycle. This metabolic pathway uses eight key enzymes and several transporters located in chloroplasts, peroxisomes, mitochondria and the cytosol. Two RuBisCO oxygenation steps are required to convert two molecules of 2-PG into a molecule of 3-PGA, with the production of one molecule of CO_2, NH_3, NADH and ADP, 2 molecules of phosphate and the consumption of an NADH and an ATP (see Bauwe *et al.*, 2010 for a review). Since this C-recycling pathway has an energetic cost, it has become a target for improving plant growth and biomass. Recently, the introduction of metabolic bypasses into the chloroplast has led to promising results with respect to increased biomass (Kebeish *et al.*, 2007; Maier *et al.*, 2012; Nölke *et al.*, 2014). Such approaches were developed because inhibiting the phosphorespiratory cycle by down-regulating a specific photorespiratory enzyme has negative effects on plant growth.

The first *Arabidopsis thaliana* photorespiratory mutants were isolated by Somerville and co-workers after screening chemically mutagenized seed (e.g. Somerville and Ogren, 1980, 1981, 1982). Since, Arabidopsis T-DNA insertion mutants of each key photorespiratory enzyme have been

isolated and characterized, thus helping to identify the corresponding photorespiratory genes (see Foyer *et al.*, 2009). In ambient air, all photorespiratory mutants are affected in their growth to differing degrees but this is not observed under high CO_2 conditions. Recently, photorespiratory phenotypes have been classified according to the severity of the symptoms: heavy (Class I, no rescue in high CO_2), strong-to-intermediate (Class II, strong growth phenotype and chlorosis in air, and after a transfer from high CO_2 to air) and intermediate-to-slight (Class III, only a slight effect on growth in air, and after a transfer from high CO_2 to air) (see Timm and Bauwe, 2013). Such observations show that the photorespiratory pathway is indispensable for normal plant growth and development. This could reflect the importance of recycling carbon from 2-PG, however photorespiration is also linked to several important metabolic processes such as photosynthesis, nitrogen-assimilation, amino acid biosynthesis, respiration, C_1-metabolism (see Foyer *et al.*, 2009; Bauwe *et al.*, 2010; Florian *et al.*, 2013). It also produces H_2O_2 (via glycolate oxidase (GO) activity) that is important in stress signaling (Foyer *et al.*, 2009). Indeed, GO mutants with less activity and H_2O_2 production have been reported to be more sensitive to pathogen attack (Rojas *et al.*, 2012). However, the effect of an altered photorespiratory capacity on plant functions is complex and poorly understood. It has already been demonstrated that net photosynthetic CO_2 assimilation is reduced in *A. thaliana* photorespiratory mutants in air (Chastain and Ogren, 1989; Takahashi *et al.*, 2007; Timm *et al.*, 2012). In certain plant species, elevated CO_2 levels or low O_2 levels that decrease photorespiration also lead to lower nitrate assimilation (Bloom *et al.*, 2010). The short-term increase of photorespiration in leaves of *X. strumarium*, by modifying the CO_2 and O_2 contents of air to modulate RuBisCO oxygenase activity, was seen to increase glycolysis and the decarboxylation rate of the TCA cycle (Tcherkez *et al.*, 2008).

An enzyme that links photorespiration to amino and organic acid metabolisms is the glutamate:glyoxylate aminotransferase (GGT; EC 2.6.1.44) that transfers an amine group from Glu to glyoxylate to produce Gly and 2-oxoglutarate. GGT is encoded by two genes in *A. thaliana*, *GGT1* (At1 g23310) and *GGT2* (At1 g70580), and although they were identified originally as homologs of alanine aminotransferases (AOAT) they show *in vitro* GGT activity, as well as Glu:pyruvate, Ala:pyruvate and Ala:2-oxoglutarate aminotransferase activities (Liepman and Olsen, 2003). GGT1 (also named AOAT1) was identified as the photorespiratory isoform because *in vitro*-grown *aoat1* knock-down plants exhibited an intermediate-slight (class III) photorespiratory phenotype that was reverted by growth in high CO_2 (Igarashi *et al.*, 2003). The phenotype could be partially reversed by low light conditions or supplementing the growth medium with 3% sucrose. *In vivo* seedling aminotransferase activities of this mutant showed an 80% decrease of Glu:glyoxylate and Ala:glyoxylate aminotransferase activities, and a 40% decrease of Ala:2-oxoglutarate and Glu:pyruvate aminotransferase activities. This mutant also contained modified amino acid levels including lower Ser and higher Glu amounts in leaves of *in vitro*-grown seedlings that were transferred from 24 h darkness to light (Igarashi *et al.*, 2003). Over-expression of *GGT1* (also named *GGAT1*) in *A. thaliana* did not result in any increase of plant biomass and growth, however Ser and Gly contents were highly increased in leaves, stems and siliques and these changes correlated with *GGT1* mRNA levels and activities (Igarashi *et al.*, 2006).

In this work, the interactions between photorespiration, photosynthesis and amino and organic acid metabolisms were investigated by studying two allelic *A. thaliana GGT1* mutant lines. Leaf primary metabolism was dissected by metabolic profiling and photosynthetic analyses of both air-grown and high CO_2 to air transferred plants. The results suggest that a low GGT activity limits rosette growth due to a limitation of carbon recycling and a low RuBisCO content that decrease leaf photosynthetic activity and impact both amino and organic acid metabolisms, so as to maintain a constant C/N balance when plants are grown in air. The observations made after transfer from high CO_2 to air give insights into the initial metabolic and physiological changes that occur and allow *ggt1* mutants to acclimate to growth in air.

RESULTS

Identification of *ggt1* T-DNA insertion lines

Two *A. thaliana* T-DNA insertion lines for *GGT1* were identified in the GABI-Kat database. Line GK-649H07 (*ggt1-1*) carries a T-DNA insertion in the second exon and line GK-847E07 (*ggt1-2*) has a T-DNA in the eighth exon of the *GGT1* coding sequence (Figure 1a). Homozygous plants for the insertion were PCR-identified. Reverse transcription-PCR of rosette leaf total RNA from air-grown *A. thaliana* Columbia (Col-0) plants confirmed *GGT1* as the major GGT gene expressed in this organ (Figure 1b). Both mutant lines showed >400-fold less *GGT1* transcripts compared to WT plants, indicating that both were indeed *ggt1* knock-out mutants. The absence of GGT1 did not lead to compensation by GGT2 since GGT2 RNA amounts did not increase in *ggt1* leaves. Rosette leaf GGT activity was reduced by >15-fold in the *ggt1* mutants when compared to the WT, consistent with the disruption of *GGT1* in both *ggt1* lines (Figure 1c). The residual GGT activity is probably due to GGT2, or other aminotransferases that exhibit low *in planta* GGT activities. Both *ggt1* mutants showed a similar slight (class III) photorespiratory phenotype (see Timm and Bauwe, 2013) since they were viable in air and only

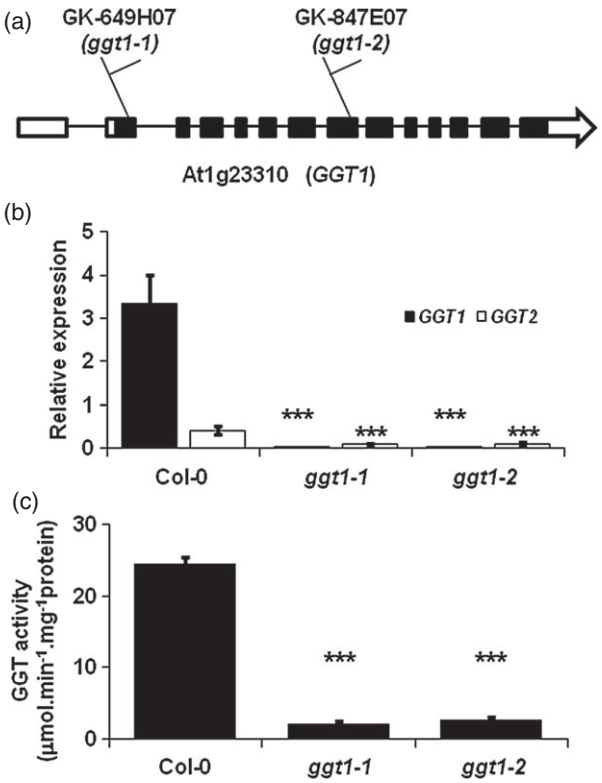

Figure 1. Identification of *A. thaliana ggt1* mutants.
(a) Localization of each T-DNA insertion in the GABI lines used in this work. Black boxes represent exons, solid lines introns and white boxes 5′ and 3′ UTR regions of At1 g23310 encoding GGT1.
(b) RT-PCR analyses of *GGT1* and *GGT2* transcripts using total RNA from 5-week-old wild type (WT) (Col-0) and *ggt1* rosette leaves. Values are normalized to the expression of *ACTIN2.* Measurements were carried out on four pools of rosette leaves.
(c) Total GGT activities of soluble extracts from six pools of 5-week-old WT and *ggt1* mutant rosette leaves. Values are means ± SD. ***Represents data that are significantly different from the Col-0 values with a Student's *t*-test ($P < 0.001$).

exhibited reduced growth in air that was not seen when they were grown in high CO_2 (Figure 2a). However, their fresh weight/dry weight ratios were unchanged compared to WT plants (Figure S1) while differences in rosette diameter and leaf number (Figure 2b,c) between *ggt1* and WT plants clearly indicated the slower growth and development of both mutants in air.

ggt1 mutants exhibit altered metabolite levels but the C/N ratio is unchanged in air-grown plants

To ensure that the observed phenotype in air resulted from a disruption of the photorespiratory pathway and to see if this perturbation affected metabolite levels of other metabolic functions, non-targeted metabolite analyses by GC-MS (Figure 3 and Table S1) and quantitative high pressure liquid chromatography (HPLC) (for amino acids, Figure 4) were carried out using 5-week-old air-grown rosette leaves of WT and both *ggt1* mutants. A five-fold increase in glyoxylate was detected in *ggt1* leaves, compared to the control (Figure 3). This finding suggested that photorespiration was indeed blocked by the reduced GGT activity in both mutants. Furthermore, there was a decrease in Ser and glycerate levels; both produced downstream from GGT in the photorespiratory cycle (Figures 3 and 4 and Table S1). Perhaps surprisingly, Gly accumulated slightly in the *ggt1* mutants (Figure 4 and Table S1). Several organic acids associated with the TCA cycle (fumarate, succinate and pyruvate) were found to decrease significantly by 1.5- to 2-fold in *ggt1* leaves (Figure 3) compared with the control while others (citrate and malate) remained unchanged (Table S1). Our non-targeted GS-MS analyses also revealed a number of other metabolite levels that were modified in both mutants compared to the WT including increases in nicotinate, phosphorate, putrescine and tyramine while *myo*-inositol decreased (Table S1). Quantitative amino acid analyses revealed a global increase of leaf soluble amino acid content in the *ggt1* mutants, but there were contrasted changes in individual amino acids (Figure 4). Ala, Arg, Asn, Asp, Gln, Glu, Gly, Val, GABA, Ile, Leu, Lys, Met, and Orn were seen to accumulate very slightly albeit significantly in both mutant lines compared with the WT, while only Ser and Thr decreased; perhaps reflecting a weak perturbation of overall amino acid metabolism (Figure 4a,b).

Analysis of leaf total carbon and nitrogen contents revealed no differences between the mutant and WT rosettes, except for a slight but significant decrease in *ggt1-1* N content. However, the leaf C/N ratio remained unchanged in the small air-grown *ggt1* plants when compared to the larger WT Col-0 plants as did nitrate and ammonium levels (Table 1). The leaves of *ggt1* mutants accumulated 35% less starch and 58% less soluble glucose at the end the day (Table 1). Total chlorophyll (chl) contents did not differ however the Chl_a/Chl_b ratio was significantly lower in both *ggt1* mutants compared to the WT. Pyridine nucleotides, and ATP and ADP contents were also measured in the different plant lines. The mutants accumulated more NADPH and less $NADP^+$ compared to the WT while NAD^+ and NADH levels did not change (Table 1). The ATP/ADP ratio also decreased in *ggt1* leaves due to the decrease of ATP levels and an increase of ADP content (Table 1).

Reduction of photosynthesis in air-grown *ggt1* mutants is independent of RuBisCO activation state

The retarded growth phenotype and the reduced starch and glucose contents of the *ggt1* plants suggested that their photosynthetic capacity might be affected. Therefore, net CO_2 assimilation rates (A_n) were measured using a home-built chamber adapted for whole plants and linked

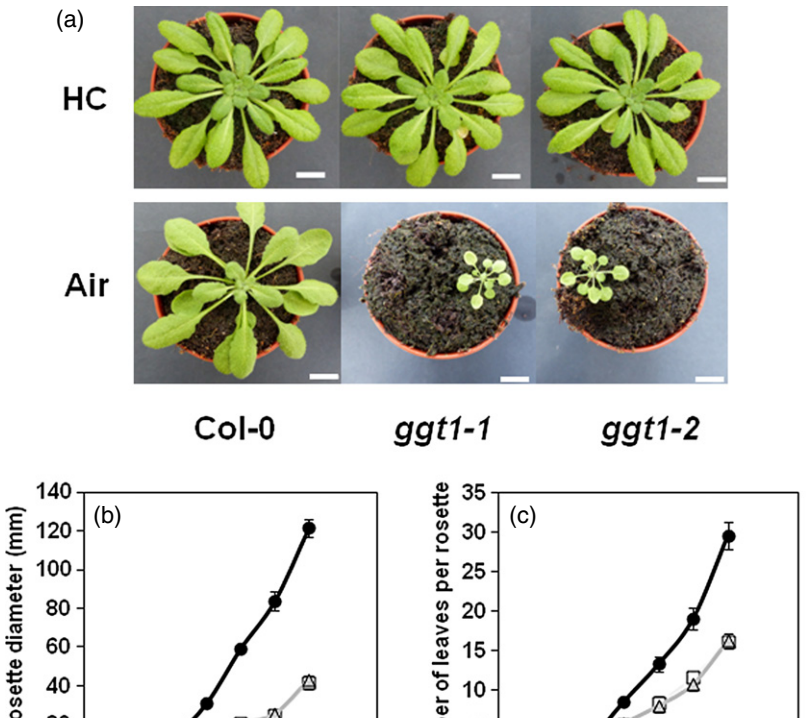

Figure 2. Growth phenotype of *ggt1* mutants.
(a) Five-week-old wild type (WT) (Col-0) and *ggt1* plants grown under short days in either high CO_2 (HC) or air. White bar = 1 cm.
(b) Rosette diameter and (c) number of leaves per rosette of *ggt1-1* (white squares), *ggt1-2* (grey triangles) and WT (black circles) plants grown under short days in air. Bars represent the standard deviation (SD) (n = 5).

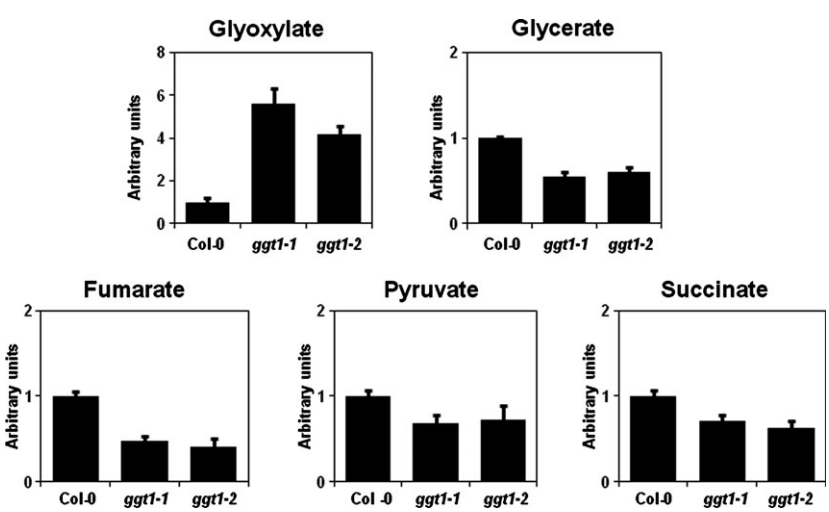

Figure 3. Significantly different relative leaf metabolite levels between air-grown wild type (WT) and *ggt1* rosettes.
Relative metabolite contents (mean ± standard deviation (SD)) are shown with the corresponding WT (Col-0) content set to 1. Bars represent the SD of three pools of 5-week-old mutant and WT leaves. All values are significantly different from the control experiment for both mutants (Student's *t*-test, $P < 0.05$, n = 3). Complete GC-MS metabolite analyses are available in Table S1.

to an infra-red gas analyzer. It was found that *ggt1* rosettes had a 45% lower A_n compared with the WT (Figure 5a). *In vitro* leaf RuBisCO activities normalized to leaf surface (to allow a comparison with the gas-exchange measurements) showed *ggt1* extracts contained significantly lower initial and total activities, but control and mutant lines exhibited similar RuBisCO activation states (Figure 5b,c). Indeed, the differences in RuBisCO activity was due to lower RuBisCO protein amounts per leaf surface in *ggt1* mutant leaves, as seen by sodium dodecyl sulphate polyacrylamide gel electrophoresis (SDS-PAGE) (Figure 5d). Such differences in RuBisCO activity would help explain the lower A_n between the WT and mutant rosettes (Figure 5a).

Physiological and metabolic analyses of plants transferred from high CO_2 conditions (non-photorespiratory) to air (photorespiratory)

In an attempt to better understand the initial changes that could have led to the air-grown photorespiratory phenotype of the *ggt1* plants it was decided to investigate the

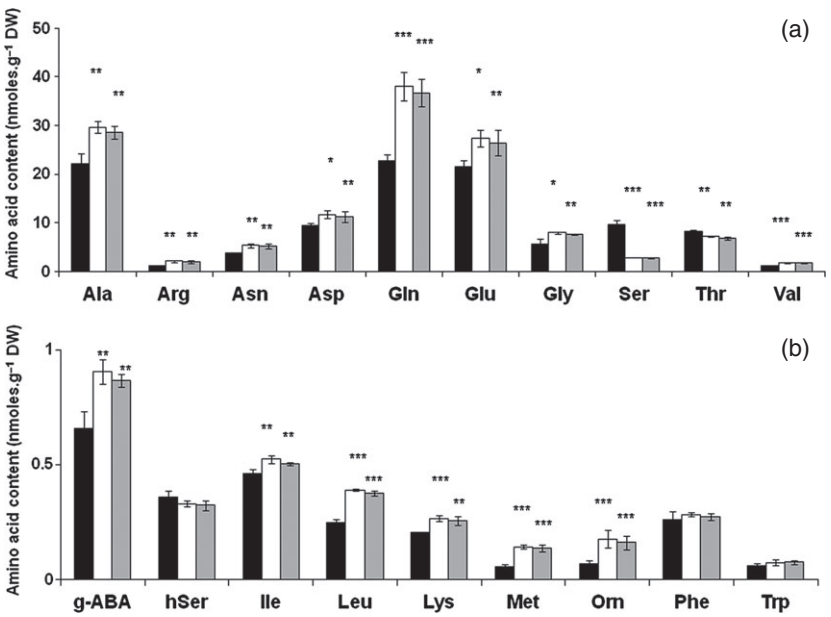

Figure 4. Soluble amino acid contents of air-grown *ggt1* and wild type (WT) rosettes.
Leaves of *ggt1* and WT plants were sampled under the light at the middle of the day and free amino acids were extracted and separated by HPLC. (a) Major and (b) minor amino acid contents of WT (black), *ggt1-1* (white) *and ggt1-2* (grey) leaves. Values are means ± standard deviation (SD) of three pools of leaves. Significantly different values from the WT are denoted (Student's *t*-test; $*P < 0.05$; $**P < 0.01$; $***P < 0.001$).

physiological and metabolic properties of plants transferred from high CO_2 (3000 μL L^{-1} for 6 weeks) to air. Gas-exchange and chlorophyll fluorescence measurements were carried out on fully expanded leaves of plants transferred to air from high CO_2 conditions for a complete 16 h night period before undertaking the analyses. Before transfer, all high CO_2 grown plants (Col-0, *ggt1-1* and *ggt1-2*) had similar A_n, dark respiration, transpiration rate, stomatal conductance, non-photochemical fluorescence quenching (NPQ) and photosynthetic electron transfer rate (ETR) values (Table S2). However, after transfer, *ggt1* leaves exhibited a steady decrease in A_n before reaching a stationary level that was 40% lower than WT rosettes after several hours (Figure 6a and Table 2). Interestingly, NPQ showed anti-parallel changes compared to A_n, with NPQ rapidly decreasing in WT leaves while remaining high in mutant rosettes (Figure 6b). The calculated ETR followed the same behavior as A_n (compare Figure 6c with Figure 6a). No differences were observed for leaf transpiration, stomatal CO_2 conductance and dark respiratory CO_2 release between WT and *ggt1* plants after their transfer to air (Table 2). When plants were placed in the dark after the light treatment, a similar rapid (10 min) dark-reversion of F_v'/F_m' was observed (Figure 6d). Taken together, these results suggest that photosynthesis is becoming progressively inhibited in *ggt1* mutants during the light period, as both CO_2 assimilation and photosynthetic electron transfer to $NADP^+$ decrease rapidly (Figure 6).

After *ggt1* mutants had attained a photosynthetic stationary-state, A_n versus CO_2 and A_n versus light intensity response curves, and the measurement of the post illumination burst (PIB) were carried out to fully characterize their CO_2 assimilatory/photorespiratory properties. The CO_2 response curve of *ggt1* plants compared to WT leaves showed that A_n was always lower in the *ggt1* leaves (espe-

Table 1 Leaf carbon, nitrogen, pyridine nucleotides, ATP and ADP contents of air-grown WT (Col-0) and *ggt1* rosettes

	Col-0	*ggt1–1*	*ggt1–2*
Total carbon (%)	35.21 ± 1.09	34.13 ± 1.94	34.24 ± 1.18
Total nitrogen (%)	6.6 ± 0.16	6.28 ± 0.16	6.48 ± 0.22
Glucose	0.83 ± 0.20	0.35 ± 0.08	0.35 ± 0.10
Starch	67.50 ± 11.50	43.77 ± 11.51	43.89 ± 10.20
Nitrate	81.79 ± 5.93	75.04 ± 7.23	79.89 ± 6.10
Ammonia	30.04 ± 4.12	32.46 ± 2.68	33.57 ± 3.67
Total Chl	1.33 ± 0.20	1.39 ± 0.26	1.43 ± 0.16
NAD^+	15.86 ± 1.67	19.99 ± 2.89	20.25 ± 2.13
NADH	1.56 ± 0.76	1.76 ± 0.22	2.17 ± 1.19
$NADP^+$	8.98 ± 1.40	7.25 ± 1.20	7.06 ± 1.41
NADPH	3.41 ± 0.79	4.50 ± 0.71	4.42 ± 0.61
ATP	137.5 ± 49.49	70.06 ± 12.83	73.62 ± 14.43
ADP	80.10 ± 16.48	123.61 ± 32.62	120.93 ± 22.85
Total C/Total N	5.33 ± 0.1	5.44 ± 0.33	5.29 ± 0.13
Chl a/Chl b	2.46 ± 0.44	1.85 ± 0.67	1.87 ± 0.59
$NADH/NAD^+$	0.10 ± 0.05	0.09 ± 0.00	0.08 ± 0.03
$NADPH/NADP^+$	0.38 ± 0.09	0.62 ± 0.06	0.64 ± 0.09
ATP/ADP	1.68 ± 0.32	0.62 ± 0.25	0.65 ± 0.25

Assays were carried out using 5-week-old air-grown rosette leaves harvested at the middle of the photoperiod, except for soluble glucose and starch contents (harvested at the end of the day). Values are the means ± SD. Significantly different values from the Col-0 data are in bold (Student's *t*-test, $P < 0.05$). Total C and N ($n = 9$); Glucose and starch ($n = 18$); Nitrate and ammonium ($n = 18$); Chl $n = 12$); Pyridine nucleotides, ATP and ADP ($n = 6$). Glucose, nitrate and ammonium, μmol g^{-1} FW; starch, μmol glucose g^{-1} FW; total chlorophyll, mg g^{-1} FW; pyridine nucleotide, ATP and ADP contents, nmoles g^{-1} FW.

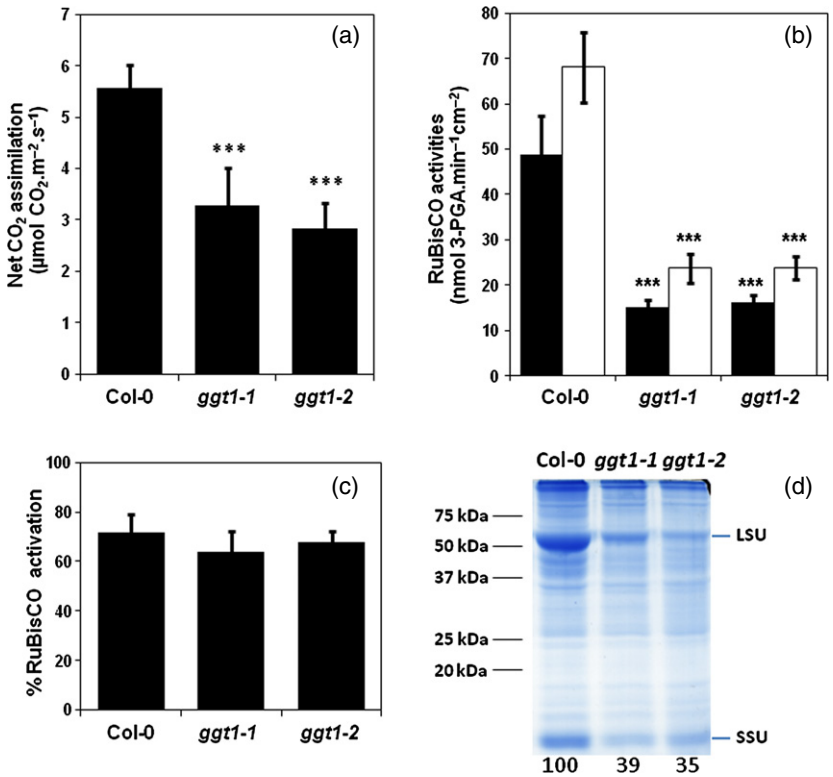

Figure 5. Net CO_2 assimilation and RuBisCO properties of air-grown wild type (WT) and *ggt1* leaves.
(a) Steady-state net CO_2 assimilation of WT (Col-0) and *ggt1* plants (at a light intensity of 200 μmol photons m^{-2} sec^{-1}).
(b) Initial (black) and total (white) RuBisCO activities.
(c) RuBisCO activation state (calculated from the initial/total activity ratio).
(d) SDS-PAGE gel showing the large (LSU) and small (SSU) RuBisCO subunits of total soluble proteins extracted from an identical leaf area (0.15 cm^2), with the corresponding intensity values for LSU relative to the WT (Col-0) normalized to 100. Values are means ± SD of either five independent plants (gas exchange) or six pools of mutant and Col-0 leaves (for activities and SDS-PAGE). Significantly different values from the WT are denoted (***, Student's *t*-test $P < 0.001$).

cially at 380 μL CO_2 L^{-1} of air) although a much smaller difference was observed in the presence of 1000 μL CO_2 L^{-1} of air (Figure S2a). The linear part of such curves (Ci range between 50 and 300 μL CO_2 L^{-1} of air) was used to calculate the CO_2 compensation point that was two-fold higher in the *ggt1* mutants compared to WT plants (Table 2). The A_n versus light response curves of *ggt1* mutants showed that A_n was not affected at low, limiting light intensities (< 50 μmol photons m^{-2} sec^{-1}) but the mutants progressively showed an enhanced inhibition of A_n as light intensity increased and CO_2 and/or RuBP recycling became limiting. At a light intensity >500 μmol photons m^{-2} sec^{-1}, A_n was nearly saturated and remained two-fold lower in both *ggt1* mutants compared to WT rosettes (Figure S2b). To ensure that photorespiration was effectively affected in the *ggt1* mutants after transfer to air, their PIB was measured. This corresponds to a continued glycine decarboxylase activity after switching off the light due to certain metabolites still being engaged in the photorespiratory pathway (Laisk and Sumberg, 1994; Kebeish *et al.*, 2007). Thus, the reduced PIB value exhibited by the *ggt1* mutants compared to WT plants (Table 2) reflects the lower photorespiratory cycle activity of these mutants. Taken together, our observations are in good agreement with a gradual inhibition of photosynthetic activity in the light when the photorespiratory cycle is inhibited in *ggt1* leaves.

It has been reported that certain photorespiratory metabolites can directly inhibit RuBisCO activity (Anderson, 1971; Lu *et al.*, 2013). Therefore, non-targeted GC-MS metabolite analyses of fully expanded rosettes leaves of WT and *ggt1* mutants were carried out before (plants in high CO_2) and after a short-term transfer to air (16 h night and 4 h day treatment) to reduce A_n in the *ggt1* leaves (Figure 7 and Table S3). As expected, a high increase of glyoxylate content (9 to 10-fold) was seen only in the transferred *ggt1* mutants (Figure 7), confirming that their photorespiratory cycle was rapidly blocked. Surprisingly, Ser content was already reduced in *ggt1* leaves before transfer to air, while decreasing further after transfer (Figure 7). Alanine and Thr were seen to decrease in both *ggt1* mutants after the transfer compared to WT plants (Table S3). Glycine was increased seven-fold in WT plants after transfer to air when compared to high CO_2 WT plants however it only increased two-fold in both *ggt1* mutants (Table S3). After a short-term transfer, the mutants did not show any differences in TCA cycle organic acids when compared to the WT (Table S3).

After the short-term transfer to air, photorespiration was reduced in the *ggt1* mutants, and this was accompanied by a decrease of A_n and photosynthetic ETR (Figure 6). The inhibition of net CO_2 assimilation could be a consequence of a direct inhibition of the RuBisCO by a photorespiratory product that accumulated in the mutant (perhaps glyoxylate in our case; Figure 7), or an inhibition of the Calvin cycle due to low ATP and NADPH levels that would impact negatively RuBP recycling to maintain RuBisCO

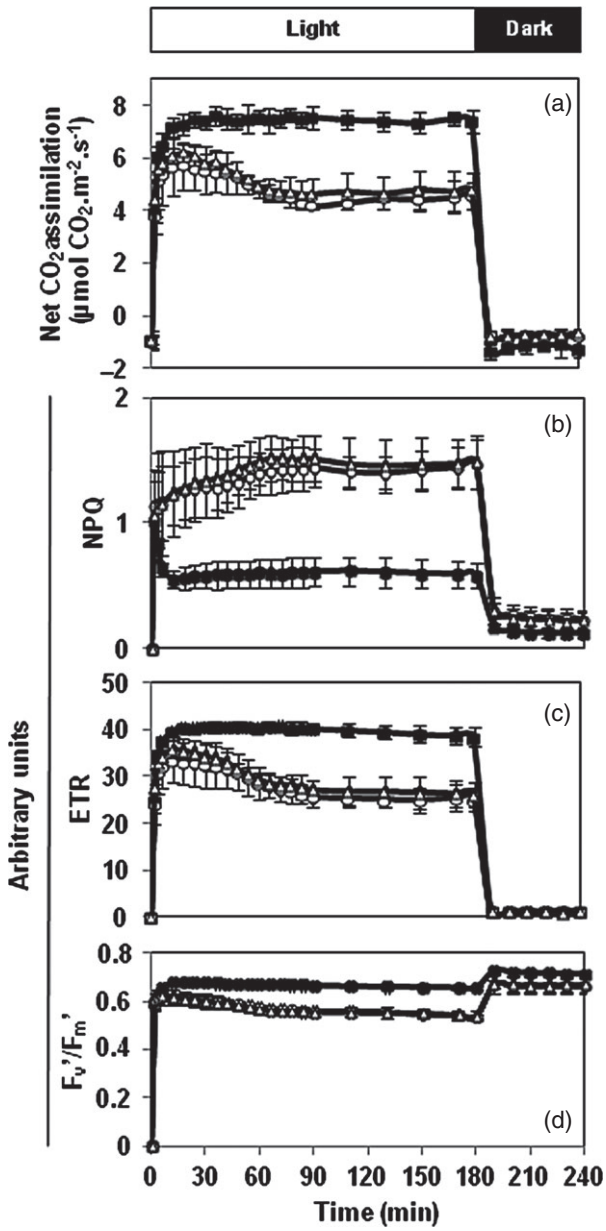

Figure 6. Changes in net CO_2 assimilation rates and chlorophyll fluorescence parameters of WT and *ggt1* rosettes after transfer from high CO_2 to air.
(a) Net CO_2 assimilation rate, (b) non-photochemical chlorophyll fluorescence quenching (NPQ), (c) photosynthetic electron transfer rate (ETR) and (d) F_v'/F_m' ratio values of WT (black squares), *ggt1-1* (white circles) *and ggt1-2* (white triangles) plants grown during 6 weeks in high CO_2 and transferred to air at the start of the night period prior to measurements the next day. Before each measurement, plants were dark-adapted for 1 h before measurements were made. Values are means ± standard deviation (SD) for three plants.

activity. Therefore, RuBisCO activities, and pyridine nucleotides, ATP and ADP contents were measured in leaf extracts before and after a short-term transfer to air. RuBisCO activities were not significantly different between *ggt1-1* and WT plants when compared either before or after this transfer, while *ggt1-2* plants always exhibited lower activities. However, slightly higher activities were seen in all transferred lines (Table 3). Furthermore, RuBisCO activation state remained constant (around 80%) for each plant line and condition (Table 3). RuBisCO amounts per leaf area were also found not to be different before and after the short-term transfer (Figure S4a), unlike in the small air-grown *ggt1* plants. No significant differences of NAD^+, NADH and NADPH contents were seen between WT and mutant leaf extracts, however slight fluctuations of $NADP^+$ levels were observed after transfer (Table 3) although $NADP^+$/NADPH ratios remained unchanged (Table 3). No differences were observed in ATP and ADP levels before transfer to air, but lower ATP and higher ADP levels were observed in the *ggt1* mutants compared to WT leaves after transfer to air; such changes reduced the ATP/ADP ratio of *ggt1* rosettes (Table 3).

It was decided to carry out a longer-term acclimation of the high CO_2 plants to air to see if *ggt1* plants became affected in their growth when compared to WT plants and whether this was associated with an altered leaf RuBisCO content (Figures 8 and S3). Leaf rosette diameter was measured during a 12 day period after transfer to air and RuBisCO levels were estimated per leaf by SDS-PAGE (Figure 8). It can be seen that several days after their transfer to air, *ggt1* rosette growth became reduced compared to the Col-0 plants (by approx. two-fold, Figure 8b) and this coincided with lower RuBisCO amounts per leaf area in the mutants (Figures 8(c) and S3b). Indeed, after transfer, RuBisCO per leaf area increased by approximately two-fold in WT plants while a significantly lower increase was observed for mutant leaves. It appears that *ggt1* leaves cannot fully acclimate to a transfer from high CO_2 to air and this leads to a slower growth that is associated with lower amounts of RuBisCO in their leaves.

DISCUSSION

The air-grown *ggt1* growth phenotype is due to a reduced A_n and less RuBisCO per leaf area

Two new mutant alleles for *A. thaliana GGT1* (Figure 1) have been characterized that exhibit a weak photorespiratory phenotype. To understand the processes underlying this phenotype, the metabolic and gas-exchange properties of air-grown mutants were compared with plants transferred from high CO_2 to air. Indeed, air-grown *ggt1* plants showed alterations in growth and development that led to smaller rosette leaves and a 10-day difference to obtain the same leaf number between 5-week-old WT and mutant plants. As expected for a photorespiratory phenotype, growth differences were not seen when plants were grown under high CO_2 conditions (Figure 2). Based on the growth phenotype and an absence of chlorosis, *ggt1* mutants show an intermediate-to-slight photorespiratory (class III)

Table 2 Physiological parameters of WT (Col-0) and *ggt1* rosettes after a short-term transfer to air

	Col-0	*ggt1–1*	*ggt1–2*
A_n (μmol CO_2 m^{-2} sec^{-1})	7.38 ± 0.44	**4.55 ± 0.51**	**4.75 ± 0.69**
R_{dark} (μmol CO_2 m^{-2} sec^{-1})	−0.77 ± 0.25	−0.81 ± 0.07	−1.01 ± 0.32
PIB (μmol CO_2 m^{-2} sec^{-1})	1.16 ± 0.14	**0.79 ± 0.11**	**0.88 ± 0.09**
CO_2 compensation point (μL CO_2 L^{-1})	51.17 ± 4.12	**101.88 ± 11.05**	**88.24 ± 12.33**
Day transpiration (mmol H_2O m^{-2} sec^{-1})	1.26 ± 0.07	1.34 ± 0.18	1.36 ± 0.17
Stomatal conductance (mmol H_2O m^{-2} sec^{-1})	0.134 ± 0.012	0.144 ± 0.0131	0.146 ± 0.0221

Net CO_2 assimilation rate (A_n), dark respiration rate (R_{dark}), post illumination burst (PIB), CO_2 compensation point, day transpiration and stomatal conductance of WT and *ggt1* rosettes grown during 6 weeks in high CO_2 and transferred to air for a night before carrying out measurements. WT and *ggt1* plants were taken the following day and values were measured after 1 h illumination. Values are means ± standard deviation (SD) ($n = 3$ for A_n, R_{dark}. day respiration and stomatal conductance; $n = 6$ for PIB and CO_2 compensation point). Values in bold are significantly different from Col-0 (Student's *t*-test, $P < 0.05$).

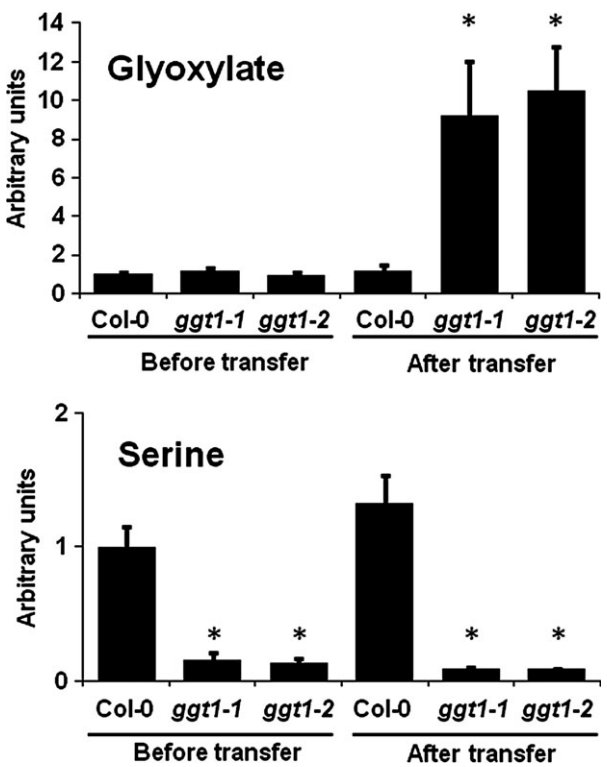

Figure 7. Serine and glyoxylate levels of wild type (WT) and *ggt1* rosettes before and after a short-term transfer from high CO_2 to air.
Plants were harvested before (at high CO_2, middle of the light period) and after transfer to air (1 night and 4 h of light). Only serine and glyoxylate levels exhibited significant differences in both *ggt1* lines compared to the WT (Col-0). Relative metabolite contents are shown with the corresponding WT content under high CO_2 set to 1. Values are means ± standard deviation (SD) for three pools of plants. Significantly different *ggt1* values compared with Col-0 before and after transfer are indicated by *Student's *t*-test, $P < 0.05$. Complete GC-MS metabolite analyses are available in Table S2.

phenotype similar to *hpr1* (see Timm *et al.*, 2012; Timm and Bauwe, 2013). The small air-grown *ggt1* plants had lower net CO_2 assimilation rates (A_n) in the light (Figure 5), which could be a major factor in the delayed growth (Figure 2). Several reasons can explain this low A_n including altered stomatal properties that reduce leaf CO_2 concentration, impaired RuBP regeneration, lower RuBisCO activation state and decreased RuBisCO protein levels. Previous analyses of another *ggt1* allele showed that the photorespiratory growth phenotype could be reverted by the addition of 3% sucrose to *in vitro*-grown mutant plantlets, suggesting that it was due to a C-limitation (Igarashi *et al.*, 2003). In this work, WT and *ggt1* plants showed several differences that could explain the low A_n. First, the accumulation of glyoxylate in the mutants (Figure 3) could affect A_n since this photorespiratory metabolite has been shown to inhibit RuBisCO light activation in isolated chloroplasts (Campbell and Ogren, 1990) and the activity of purified spinach RuBisCO (Cook *et al.*, 1985). In contrast, glyoxylate appeared to inhibit RuBP regeneration without affecting RuBisCO activation and activity in spinach chloroplasts (Mulligan *et al.*, 1983). In *A. thaliana*, a correlation has been made between glyoxylate accumulation and the A_n decrease of several photorespiratory mutants (previously named *stm*, *dct*, *glyD*, *gluS*, *sat*) in 50% O_2-air in the light that was attributed to either a decrease in RuBisCO activation or reduced RuBP regeneration or both depending on the mutant (Chastain and Ogren, 1989). Recently, the analysis of air-grown rice plants with reduced GO activities exhibiting a lower A_n was attributed to a reduced RuBisCO activation state (Xu *et al.*, 2009) and correlated with unexpected high glyoxylate levels (Lu *et al.*, 2013). In our work, no changes in RuBisCO activation state were found in air-grown *ggt1* plants compared to the WT (Figure 5). Conversely, both RuBisCO activity and content per leaf surface were three-fold lower in air-grown *ggt1* leaves compared to WT rosettes (Figure 5). Interestingly, an *A. thaliana rbsc1a3b-1* mutant deficient in two RuBisCO small subunit isoforms showed a delayed growth similar to *ggt1* that was associated with leaves containing 30% WT RuBisCO amounts and a three-fold lower A_n, without any modification in stomatal conductance (Izumi *et al.*, 2012). Similar changes were found also in anti-sensed *rbcS*

Table 3 RuBisCO activities, and pyridine nucleotide, ATP and ADP contents of WT and *ggt1* leaves before and after a short-term transfer from high CO_2 to air

	Before transfer			After transfer		
	Col-0	*ggt1–1*	*ggt1–2*	Col-0	*ggt1–1*	*ggt1–2*
Initial RuBisCO activity	21.87 ± 4.01	18.18 ± 1.95	**15.7 ± 1.06**	32.21 ± 7.79	25.51 ± 3.7	**21.88 ± 3.01**
Total RuBisCO activity	25.86 ± 3.57	23.31 ± 1.93	**19.03 ± 2.03**	38.75 ± 6.1	32.12 ± 4.37	**27.5 ± 1.98**
RuBisCO activation (%)	84.33 ± 7.2	78.02 ± 5.65	82.95 ± 6.09	82.48 ± 9.26	79.52 ± 5.52	79.41 ± 7.36
NAD^+	14.16 ± 3.36	15.73 ± 1.21	13.92 ± 2.98	16.07 ± 4.41	18.64 ± 4.81	18.95 ± 4.24
NADH	0.77 ± 0.36	0.80 ± 0.16	0.98 ± 0.40	1.40 ± 0.31	1.21 ± 0.50	1.41 ± 0.42
$NADP^+$	7.14 ± 1.30	7.31 ± 1.48	6.86 ± 1.54	9.60 ± 1.95	**6.70 ± 1.04**	**7.51 ± 1.17**
NADPH	6.35 ± 2.19	5.68 ± 1.66	7.12 ± 1.81	8.46 ± 2.60	6.23 ± 1.16	7.48 ± 1.51
ATP	232.8 ± 50.2	193.6 ± 70.1	236.0 ± 88.3	341.7 ± 57.9	**222.3 ± 96.5**	**273.4 ± 32.0**
ADP	167.3 ± 56.2	184.5 ± 107.5	174.4 ± 62.5	98.8 ± 45.0	**181.8 ± 47.2**	151.6 ± 43.5
$NADH/NAD^+$	0.06 ± 0.03	0.05 ± 0.01	0.07 ± 0.04	0.09 ± 0.03	0.07 ± 0.03	0.08 ± 0.04
$NADPH/NADP^+$	0.91 ± 0.36	0.84 ± 0.46	1.11 ± 0.44	0.91 ± 0.32	0.95 ± 0.19	1.00 ± 0.17
ATP/ADP	1.60 ± 0.94	1.29 ± 0.75	1.54 ± 0.82	3.88 ± 1.26	**1.39 ± 1.02**	**1.90 ± 0.47**

Assays were made on rosette leaf extracts of plants grown in high CO_2 for 6 weeks prior to transfer to air for a night before harvesting the leaves at the middle of the following day. Values are means ± standard deviation (SD) ($n = 6$). Significantly different values from Col-0 are in bold (Student's *t*-test, $P < 0.05$). RuBisCO activities, nmoles 3-PGA min^{-1} cm^{-2}; pyridine nucleotide, ATP and ADP contents, nmoles g^{-1} FW.

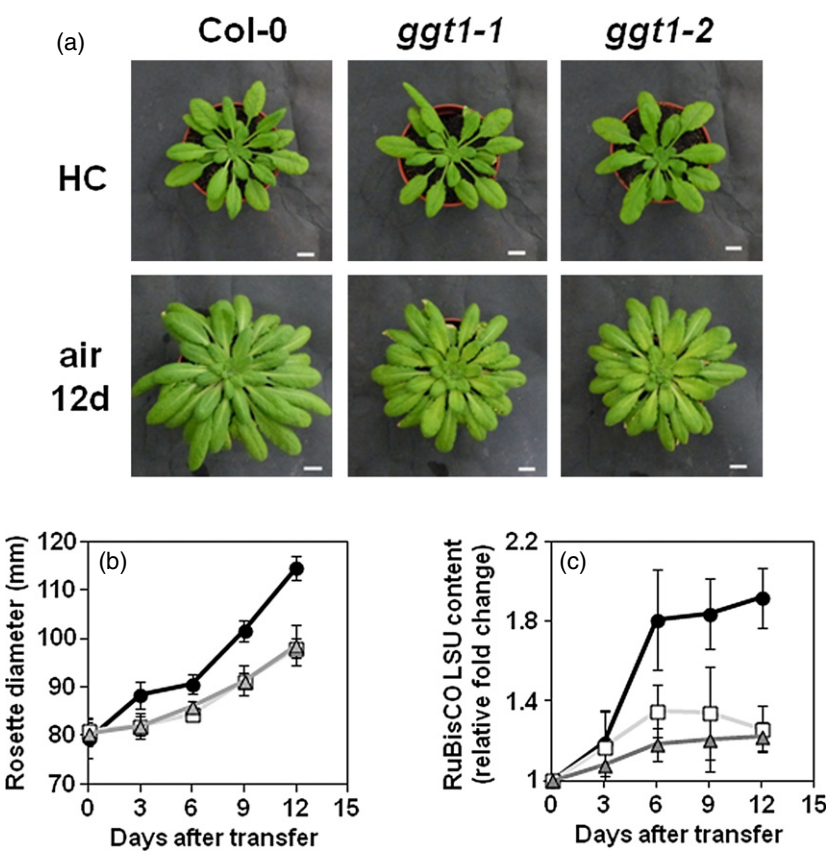

Figure 8. Growth phenotype and RuBisCO large subunit amounts during a long-term transfer from high CO_2 to air.
Twelve days after transfer to air (12 days) from high CO_2 (HC), *ggt1* rosettes showed reduced growth compared to WT rosettes (a). Changes in rosette diameter (b) and RuBisCO large subunit (LSU) contents (c) were measured before (0) and after transfer to air (3, 6, 9 and 12 days). RuBisCO amounts are relative to the 0-day values for each plant line.

tobacco plants containing less RuBisCO, although RuBisCO activity had to decrease below 60% before growth phenotypes occurred. At around 65% inhibition, the plants showed a 50% inhibition of A_n, reduced biomass and leaf size and no change in C/N ratio (Quick *et al.*, 1991) In rice, RuBisCO anti-sensed lines with 30% WT RuBisCO content per leaf surface also showed a decrease in A_n and relative growth rate (Sudo *et al.*, 2014). These observations clearly

suggest that the lower amount of RuBisCO per leaf surface is responsible for the lower A_n and reduced growth of air-grown *ggt1* mutants. Reduced RuBisCO levels can explain also the 40% decrease in total soluble leaf protein content per surface in the mutants (calculated from Figure S1).

Low RuBisCO amounts and an inhibited photorespiratory cycle have a significant impact on primary metabolism of air-grown *ggt1* plants

The reduction in starch and glucose at the end of the day probably reflects a limitation in C-assimilation (due to the low A_n and RuBisCO content) and/or photorespiratory C-recycling (due to the *ggt1* mutation). However, similar results were observed for starch and sucrose contents of rice leaves with less RuBisCO (Sudo *et al.*, 2014) perhaps suggesting that our changes are due to the decreased A_n. In addition, *ggt1* mutants showed lower TCA cycle-related organic acids (pyruvate, fumarate and succinate), perhaps indicating a reallocation of carbon due to a long-term adaption response to the low C-assimilation rate since such changes were not observed in the short-term transferred plants (Figure 3 and Table S2). A reduced TCA cycle activity would impact respiratory ATP synthesis due to a lower mitochondrial NADH production that could explain, in part, the reduction in the ATP/ADP ratio observed in air-grown *ggt1* rosettes (Table 1). Less ATP in the mutants might also reflect a lower chloroplastic ATPase activity since anti-sensed tobacco lines for this enzyme show a low A_n associated with high NPQ values (Rott *et al.*, 2011). However, the rosette leaves of WT and air-grown mutants showed no differences in NPQ (Figure S4). It is probable that the lower ATP/ADP and $NADP^+$/NADPH ratios of the *ggt1* leaves reflect the long-term acclimation of plant metabolism to the low A_n.

Some of the observed metabolite changes in the air-grown plants could be associated easily with the reduced GGT activity. The substrates of this aminotransferase were both affected; glyoxylate accumulated several fold while Glu increased significantly (Figures 3 and 4 and Table S1). Alanine levels were increased in *ggt1* leaves and this could reflect the Ala:glyoxylate aminotransferase activity of GGT (Igarashi *et al.*, 2003). However, higher Ala and lower pyruvate levels could be due to a modified C-allocation towards certain amino acid biosynthetic pathways. A reduction of photorespiratory metabolites downstream of the mutation (Ser and glycerate) was also observed (Figures 3 and 4 and Table S1). Surprisingly, Gly content increased slightly (Figure 4 and Table S1) thus suggesting the involvement of non-photorespiratory pathways to maintain Gly levels in the air-grown mutants. Perhaps *in vivo* Ser:glyoxylate aminotransferase (SGAT) activity was increased compared with the WT due to high glyoxylate levels, thus decreasing Ser content to produce Gly. It is possible also to produce Gly from Thr via threonine aldolase (THA). *A. thaliana* mutants of *THA1* and *THA2* show an increase in leaf Thr content and a decrease in Gly and Ile contents (Joshi *et al.*, 2006) and similar changes were observed in the *ggt1* mutants (Figure 4 and Table S1). Glycine can also be produced from Ser by mitochondrial or non-mitochondrial SHMT activities (Bauwe and Kolukisaoqlu, 2003), while Ser can be produced by non-photorespiratory pathways from 3-PGA (Ros *et al.*, 2014). The low Ser levels and slightly increased Gly levels in *ggt1* leaves could highlight the importance of maintaining Ser-Gly recycling for C_1 metabolism and the multitude of linked biosynthetic reactions including Met biosynthesis (it should be noted that Met levels were doubled in the *ggt1* plants compared with the WT, see Figure 4). Indeed, Gly decarboxylase P-protein mutants are lethal and they cannot be recovered in high CO_2 thus indicating the importance of Ser-Gly cycling (Engel *et al.*, 2007). In general, *ggt1* leaves contained higher soluble amino acid levels (on a dry weight basis) therefore indicating a modification of amino acid metabolism in air-grown *ggt1* plants. That said, both nitrate and ammonia pools were not seen to change (Table 1) even though low photorespiratory conditions have been reported to inhibit nitrate uptake and assimilation in *A. thaliana* (Rachmilevitch *et al.*, 2004; Bloom *et al.*, 2010). Perhaps, the observed changes reflect the lower amounts of protein in the mutants (Figure S1) thus leading to a general increase in soluble amino acid levels (Figure 4). Albeit the metabolic differences between *ggt1* and WT leaves, leaf C/N ratio was not altered in 5-week-old air-grown plants (Table 1). It appears that *ggt1* plants have acclimated their growth, development and metabolism to maintain C/N homeostasis. This was also seen for tobacco plants with similar low RuBisCO levels (Quick *et al.*, 1991). In order to try to decipher the initial events occurring in *ggt1* leaves that trigger the long-term acclimation responses, plants transferred from high CO_2 to air were analyzed.

A short-term transfer of *ggt1* plants from high CO_2 to air leads to A_n inhibition without altering RuBisCO properties

Before transfer from high CO_2 to air, *ggt1* mutants showed no growth phenotype compared to WT plants (Figure 2). RuBisCO levels, activities and activation state were also similar to the WT (Table 3 and Figure S3a,b), suggesting that reduction of the RuBisCO oxygenase activity in high CO_2 was sufficient to inhibit the changes observed in air-grown mutants. Although metabolite levels were also similar, surprisingly, Ser content was found to be decreased by 85% in both *ggt1* lines compared to the WT before transfer (Figure 7). Recently, the phosphorylated Ser biosynthesis pathway has been shown to be important for Ser content under low photorespiratory conditions since a 3-PGA dehydrogenase mutant (*pgdh1*) produced 50% less Ser under these conditions, and showed a growth phenotype (Benstein *et al.*, 2013). It is therefore surprising

that high CO_2 grown *ggt1* plants mutants still exhibit a severe reduction of Ser content (Figure 7) but do not show a similar *pgdh1*growth phenotype, thus suggesting that the observed phenotype in the *pgdh1* mutants might not be due to low Ser levels. Furthermore, it appears that the low Ser content of our *ggt1* mutants is not due to the photorespiratory role of GGT but to an undetermined modification of Ser homeostasis that is independent of the photorespiratory cycle. After transfer to air, A_n was seen to rapidly decrease to 63% of the WT value, NPQ increased to attain a high steady-state level while photosynthetic ETR mirrored the decrease in A_n (Figure 6). The decrease in A_n was not accompanied by either changes in RuBisCO properties or stomatal conductance (Table 3 and Figure S3). Earlier identified *A. thaliana* photorespiratory mutants were seen also to show a similar decrease in A_n in the light, but at high photorespiratory conditions (50% O_2) (Somerville and Ogren, 1980, 1981, 1982; Chastain and Ogren, 1989). Several of these photorespiratory mutants were characterized also at 21% O_2 and they showed a decrease in A_n with an increase in NPQ after a transfer from high CO_2 to air. Furthermore, the excess absorbed light resulted in an inhibition of photosystem 2 (PS2) D1 protein synthesis leading to photoinhibition (Takahashi *et al.*, 2007). NPQ is associated with high energy state thermal dissipation induced by a pH gradient across the thylakoid membrane, changes in light harvesting antenna distribution between the two photosystems called state 1–state 2 transitions, and PS2 damage leading to photoinhibition. The latter two processes are associated with dark relaxation times of 10 min to several hours, whereas the pH gradient is rapidly reversed within 1–2 min (see Hodges *et al.*, 1989 and Horton *et al.*, 1996), therefore the rapid dark-induced changes in F_v'/F_m' indicate that no photoinhibition was occurring under our conditions (Figure 6). High NPQ values are associated with low CO_2 assimilation rates and Calvin cycle activities since the non-dissipation of the pH gradient slows photosynthetic ETR and thus decreases NADPH and ATP production, reducing light activation of Calvin cycle enzymes by thioredoxins (Dai *et al.*, 2004), and RuBP recycling. Therefore, the high NPQ state of *ggt1* leaves in the light clearly indicates a notable disequilibrium between light absorption, photosynthetic ETR, CO_2 assimilation, and RuBP recycling. Since RuBisCO levels, extractable activities and activation state did not differ between the short-term transferred *ggt1* and WT plants (Table 3 and Figure S3), we propose that our data fit better with a defect in RuBP recycling due to the reduction in photorespiratory C-recycling observed in *ggt1* leaves as highlighted by the increase in glyoxylate levels (Figure 7). Since changes in ETR mirror those of A_n in transferred *ggt1* plants, the $NADPH/NADP^+$ ratio might be expected not to change significantly while the continuous high pH gradient would reduce ATP synthesis and lower the ATP/ADP ratio (Table 3). Finally, TCA cycle organic acid contents (Table S2), and dark respiration rate (Table 2) were not different between WT and *ggt1* plants after the short-term transfer, suggesting that altered C-allocation to the TCA cycle is not a short-term response to C-limitation and therefore the differences in ATP/ADP ratio after transfer do not appear to be linked to mitochondrial respiration.

Interestingly, after a longer-term acclimation after transfer from high CO_2 to air the *ggt1* leaves began to exhibit a reduced growth rate when compared to WT plants (Figure 8). This was accompanied by differences in leaf RuBisCO levels between the mutant and Col-0 plants (Figures 8c and S3b). Thus, such observations are in agreement with the idea that *ggt1* growth in air becomes limited by the reduced photosynthetic capacity of the mutant leaves that eventually has a negative impact on RuBisCO amounts.

In conclusion, we have shown that the photorespiratory phenotype of air-grown *A. thaliana ggt1* mutants is initially the result of a reduction in photorespiratory C-recycling, leading to a large increase in glyoxylate that rapidly affects leaf photosynthetic properties. As a consequence, RuBisCO fixes less CO_2, resulting in a C-limitation that impacts N-assimilation, thus further decreasing RuBisCO content. This negative feedback cycle continues until *ggt1* plants attain a new homeostatic state that maintains a constant C/N balance. The need to balance plant N demand with available assimilated C produces smaller, slower growing plants.

EXPERIMENTAL PROCEDURES

Material and growth conditions

Studies were carried out with *A. thaliana* wild-type (WT) plants ecotype Columbia (Col-0) and T-DNA mutants of *GGT1* (At1 g23310), GK-649H07 (*ggt1-1*) and GK-847E07 (*ggt1-2*) obtained from GABI-Kat (University of Bielefeld, Bielefeld, Germany). Plants were grown in air (380 μL CO_2 L^{-1} air) or high CO_2 (3000 μL CO_2 L^{-1} air), under a 8 h light/16 h dark cycle (20°C/18°C), in growth chambers (at 200 μmol photons m^{-2} sec^{-1} of light intensity) on commercial peat substrate fertilized with 1 kg m^{-3} of a 17:10:14 nitrogen/phosphate/potassium mix. Transfer experiments were carried out on 6-week-old WT and *ggt1* plants grown in high CO_2 and transferred to air for the night prior to a 4 h light (200 μmol photons m^{-2} sec^{-1}) treatment (short-term) or for up-to-12 days (long term at 350 μmol photons m^{-2} sec^{-1}) before being frozen in liquid nitrogen and stored. For air-grown plant analyses, 15 *ggt1* rosettes were pooled for each extraction. Five-week-old plants were taken at the middle of the photoperiod and frozen in liquid nitrogen and stored.

Isolation of T-DNA mutants and quantitative RT-PCR

PCR-based screening was used to isolate homozygous T3 T-DNA insertion lines for *ggt1-1* and *ggt1-2.* Primers P1, P2, P3, P4, P5 and P6 were used for genomic DNA screening (for primer sequences, see Table S4). Genomic DNA was extracted as in Edwards *et al.*, 1991. The primers used for amplification of the WT gene were P1-P2 for *ggt1-1* and P5-P6 for *ggt1-2.* Primers used for

T-DNA/gene junction amplification were P3-P4 for *ggt1-1* and P4-P5 for *ggt1-2*. Total RNA was obtained by TRIzol® extraction of 200 mg frozen powdered 5-week-old rosette leaves. After a DNase treatment of 1 μg extracted RNA, 500 ng of RNA were taken for reverse transcription according to the supplier's protocol (Promega, Charbonniers, France). The resulting cDNAs were diluted three-fold for quantitative PCR analysis using SYBR green and a Light Cycler 480 Real-Time PCR System (Roche Diagnostics, Mannheim, Germany). The primers for *GGT1* and *GGT2* amplification were P7-P8 and P9-P10, respectively. *GGT* transcript levels were normalized to *ACTIN 2* (P11 and P12 primers).

Rosette leaf enzymatic activities

For GGT activities, after grinding frozen material to a fine powder, leaf proteins were extracted in 100 mM Tris-HCl (pH 7.3) containing an anti-protease cocktail (Complete-Mini, Roche Diagnostics, Mannheim, Germany). The suspension was centrifuged 20 000 ***g*** for 10 min at 4°C, and 0.5 mL of each supernatant was desalted by filtration on a NAP-5 column (GE Healthcare, Chalfont St Giles, UK). GGT activity was measured spectrophotometrically by monitoring NADH oxidation at 340 nm in a mixture containing 100 mM Tris–HCl (pH 7.3), 20 mM glutamate, 1 mM glyoxylate, 0.18 mM NADH, 83 mM NH_4Cl and 0.3 U glutamate dehydrogenase and 230 μg of extracted soluble proteins. RuBisCO activity was carried out using leaf soluble proteins extracted at 4°C with degasified 100 mM Bicine, pH 8. After a short spin (10 sec) the supernatant was used for activity measurements as described in Ward and Keys (1989). For total RuBisCO activity, 25 μg of extracted soluble proteins were incubated with 10 mM $NaHCO_3$ and 20 mM $MgCl_2$ for 10 min before adding 660 μM RuBP. For initial RuBisCO activities, $NaHCO_3$ and $MgCl_2$ were added after the RuBP. Leaf soluble protein levels were calculated using the Bradford reagent (Sigma-Aldrich Chimie, St Quentin Fallavier, France) with bovine serum albumin as the standard.

Gas-exchange measurements

After transfer, a fully expanded leaf was placed in a gas-exchange chamber (LCF 6400-40, LiCOR, Lincoln, NE, USA) connected to a portable photosynthesis system (LI 6400XT, LiCOR, Lincoln, Nebraska, USA). Standard measuring conditions were: 200 μmol photons m^{-2} sec^{-1} of light intensity, a leaf temperature of 21°C, 60–70% relative humidity (VPD leaf approximately equal to 1), 380 μL CO_2 L^{-1} and 0.21 L O_2 L^{-1}. Measurements were also carried out at 1900 μL CO_2 L^{-1} to examine high CO_2 grown WT and mutant plants before transfer to air. Chlorophyll fluorescence parameters were measured using the leaf fluorescence chamber and calculated as follows (see Maxwell and Johnson, 2000): $F_v = F_m - F_o$, $F_v' = F_m' - F_o'$, $NPQ = (F_m - F_m')/ F_m'$, $ETR = ((F_m' - F_v)/ F_m')0.5*I*\alpha_{leaf}$ with I corresponding to the irradiance in μmol photons m^{-2} sec^{-1} and α_{leaf} to the light absorption coefficient of a leaf (= 0.85; see Peterson and Havir, 2001). Plants were adapted 30 min to darkness before measuring the F_0 and F_m levels. After illumination, measurements were taken during 3 h and for a further 1 h after being placed in the dark. For A_n/c_i curves and A_n/PAR_{in} curves, plants were light acclimated for 1 h at 380 μL L^{-1} CO_2 to allow *ggt1* mutants to attain a stationary A_n level. The CO_2 concentrations used were 100, 200, 300, 400, 600, 800, 1000, and 1200 μL CO_2 L^{-1} and for Col-0, 50 μL CO_2 L^{-1} was added. CO_2 compensation points were calculated by regression analyses of the linear range of the curve (100 to 400 μL.L^{-1}). PAR_{in} values used for all genotypes were 0, 25, 50, 100, 150, 200, 250, 500, 750, 1000, 1250, 1500, and 1750 μmol photons m^{-2} sec^{-1}. The PIB was measured after a 30 min adaption of plants at 100 μL CO_2 L^{-1} and 1000 μmol photons m^{-2} sec^{-1}, before turning off the light for 10 min (Laisk and Sumberg, 1994; Kebeish *et al.*, 2007). The transient CO_2 peak was recorded every 2 sec.

Metabolite analyses by GC-MS and HPLC

Rosette leaves were lyophilized for 96 h, and ground to a fine powder. Metabolites were extracted with cold methanol. Amino acids were quantified by HPLC and relative metabolite levels were analyzed by GC- MS according to Noctor *et al.*, 2007.

Chlorophyll contents

Chlorophylls were acetone-extracted from finely ground leaf material and chlorophyll contents were calculated from absorbance values at 663 nm and 646 nm according to Porra *et al.*, 1989.

Nitrate and ammonia contents

Fifty milligrams of finely ground frozen material was re-solubilized with 1 mL extraction buffer containing 100 mM HCl and 0.2% polyvinylpyridine. After centrifugation, 10 min at 10 000 ***g*** and 4°C, the resulting supernatant was used for each assay. Nitrate amounts were calculated from the absorbance values at 410 nm, following the formation of nitrosalicylate ion according to Cataldo *et al.* (1975). For ammonia quantification, 10 μL of supernatant was mixed with 0.5 mL of 0.33 M sodium phenolate (pH 13), 0.5 mL of 1.5% NaClO and 0.5 mL of H_2O and incubated for 1 h at room temperature. The ammonia-derived indophenol was quantified spectrophotometrically at 635 nm.

Soluble glucose and starch contents

One hundred milligrams of frozen material was re-solubilized in 1 mL of 1 M $HClO_4$ at 4°C. After a 5 min centrifugation at 10 000 ***g*** and 4°C, the supernatant was transferred to a new tube and the pellet was kept for starch detection. Supernatants were adjusted to pH 7 using a buffer containing Tris 0.5 M pH 7.5 and 5 M K_2CO_3 and centrifuged for 5 min at 10 000 ***g*** and 4°C. The resulting supernatant was used to measure soluble glucose. The pellets were dried 2 h at 50°C, resuspended in 1 mL of deionised water and incubated for 2 h at 100°C. After adjusting the pH to 7 by adding approximately 500 μL of 200 mM acetate-sodium buffer, pH 4.8, starch was digested to glucose overnight at 60°C by the addition of 0.5 U amyloglucosidase. Glucose contents were measured using the R-Biopharm kit (Boehringer Mannheim, Darmstadt, Germany) by following the manufacturer's instructions.

Pyridine nucleotide, ATP and ADP contents

Reduced and oxidized pyridine nucleotides were measured from soluble leaf extracts as previously described (Queval and Noctor, 2007). For ATP and ADP measurements, 100 mg of rosette leaves from WT and *ggt1* plants were extracted with 0.5 mL of 2.3% trichloroacetic acid. After a 30 min centrifugation at 16 000 ***g*** and 4°C, the supernatant was adjusted to pH 7 with 1 mL of 100 mM Tris–acetate buffer pH 7.75. ATP was directly quantified by luminescence using a luciferase ATP detection assay kit (ABCAM, Paris, France). ADP was converted to ATP for 10 min at room temperature using 1 U pyruvate kinase, 1 mM PEP, 12.5 mM KCl_2 and 25 mM $MgCl_2$. The additional ATP detected corresponded to the ADP in the extract.

Total carbon and nitrogen contents

Two milligrams of lyophilized frozen material were burned in an elemental analyser (Pyrocube, Elementar, Lyon, France) and the

resulting N_2 and CO_2 gas quantified by isotopic mass spectrometry against standards (ammonium sulfate (N1IAEA and N2IAEA) 21.2% N, acetanilide 10.36% N and 71.09% C, glutamic acid (AGIAEA USGS40) 9.51% N and 40.82% C).

RuBisCO amounts by SDS-PAGE

Leaves were harvested at the middle of the photoperiod and their leaf area measured (using ImageJ software) before being frozen and ground to a fine powder. Soluble proteins were extracted in 100 mM Bicine, pH 8 supplemented with an anti-protease cocktail (Complete-Mini, Roche Diagnostics, Mannheim, Germany) to give a leaf surface per volume ratio of either 10 cm^2 mL^{-1} (long-term acclimation experiments) or 5 cm^2 mL^{-1} (air-grown plants). Proteins were separated on SDS-PAGE gels (10% acrylamide) and proteins were detected by Coomassie blue staining as in Laemmli (1970). The amount of RuBisCO large subunit per leaf area was quantified from stained gels using ImageJ software.

ACKNOWLEDGEMENTS

This work is supported by a public grant overseen by the French National Research Agency (ANR) as part of the 'Investissement d'Avenir' programme, through the 'Lidex-3P' project and a French State grant (ANR-10-LABX-0040-SPS) funded by the IDEX Paris-Saclay, ANR-11-IDEX-0003–02. YD was supported by a PhD grant from the French Ministry of Higher Education and Research. We would like to thank Françoise Gilard and Caroline Mauve of the Institute of Plant Sciences Paris-Saclay Métabolisme-Métabolome facility for their help with the GC-MS and HPLC analyses and Céline Masclaux-Daubresse (Institut Jean-Pierre Bourgin, INRA, Versailles) for her help with the whole-plant chlorophyll fluorescence measurements.

SUPPORTING INFORMATION

Additional Supporting Information may be found in the online version of this article.

Figure S1. Leaf weights and soluble protein levels of WT and *ggt1* plants grown in either air or high CO_2.

Figure S2. Response of A_n to CO_2 and light in WT and *ggt1* leaves after a transfer from high CO_2 to air.

Figure S3. Relative RuBisCO amounts per leaf surface of WT and *ggt1* leaves before and after a transfer from high CO_2 to air and the development of a slight photorespiratory growth phenotype.

Figure S4. Non-photochemical fluorescence quenching of air-grown WT and *ggt1* rosettes.

Table S1. Relative metabolite levels of air-grown WT and *ggt1* leaves.

Table S2. Gas exchange and chlorophyll fluorescence parameters of high CO_2 grown WT (Col-0) and *ggt1* rosettes measured in CO_2-enriched air.

Table S3. Relative metabolite levels of WT and *ggt1* leaves before after a short-term transfer from high CO_2 to air.

Table S4. Primers used in this work.

REFERENCES

Anderson, L.E. (1971) Chloroplast and cytoplasmic enzymes II. Pea leaf triose phosphate isomerases. *Biochim. Biophys. Acta*, **235**, 237–244.

Bauwe, H. and Kolukisaoqlu, U. (2003) Genetic manipulation of glycine decarboxylation. *J. Exp. Bot.* **54**, 1523–1535.

Bauwe, H., Hagemann, M. and Fernie, A.R. (2010) Photorespiration: players, partners and origin. *Trends Plant Sci.* **15**, 300–336.

Benstein, R.M., Ludewig, K., Wulfert, S., Wittek, S., Gigolashvili, T., Frerigmann, H., Gierth, M., Flügge, U.-I. and Krueger, S. (2013) Arabidopsis phosphoglycerate dehydrogenase 1 of the phosphoserine pathway is essential for development and required for ammonium assimilation and tryptophan biosynthesis. *Plant Cell*, **25**, 5011–5029.

Bloom, A.J., Burger, M., Rubio Asensio, J.S. and Cousins, A.B. (2010) Carbon dioxide enrichment inhibits nitrate assimilation in wheat and Arabidopsis. *Science*, **328**, 899–903.

Campbell, W.J. and Ogren, W.L. (1990) Glyoxylate inhibition of ribulosebisphosphate carboxylase/oxygenase activation in intact, lysed and reconstituted chloroplasts. *Photosynth. Res.* **23**, 257–268.

Cataldo, D.A., Maroon, M., Schrader, L.E. and Youngs, V.L. (1975) Rapid colorimetric determination of nitrate in plant tissues by nitration of salicylic acid. *Commun. Soil Sci. Plant Anal.* **6**, 71–80.

Chastain, C.J. and Ogren, W.L. (1989) Glyoxylate inhibition of ribulosebisphosphate carboxylase/oxygenase activation state *in vivo*. *Plant Cell Physiol.* **30**, 937–944.

Cook, C.M., Mulligan, R.M. and Tolbert, N.E. (1985) Inhibition and stimulation of ribulose-1,5-bisphosphate carboxylase/oxygenase by glyoxylate. *Arch. Biochem. Biophys.* **240**, 392–401.

Dai, S., Johansson, K., Miginiac-Maslow, M., Schürmann, P. and Eklund, H. (2004) Structural basis of redox signaling in photosynthesis: structure and function of ferredoxin:thioredoxin reductase and target enzymes. *Photosynth. Res.* **79**, 233–248.

Edwards, K., Johnstone, C. and Thompson, C. (1991) A simple and rapid method for the preparation of plant genomic DNA for PCR analysis. *Nucl. Acid. Res.* **19**, 1349.

Engel, N., van den Daele, K., Kolukisaoqlu, U., Morgenthal, K., Weckwerth, W., Pärnik, T., Keeberg, O. and Bauwe, H. (2007) Deletion of glycine decarboxylase in Arabidopsis is lethal under nonphotorespiratory conditions. *Plant Physiol.* **144**, 1328–1335.

Florian, A., Araujo, W.L. and Fernie, A.R. (2013) New insights into photorespiration obtained from metabolomics. *Plant Biol.* **15**, 656–666.

Foyer, C.H., Bloom, A.J., Queval, G. and Noctor, G. (2009) Photorespiratory metabolism: genes, mutants, energetic, and redox signaling. *Annu. Rev. Plant Biol.* **60**, 455–484.

Hodges, M., Cornic, G. and Briantais, J.-M. (1989) Chlorophyll fluorescence from spinach leaves: resolution of non-photochemical quenching. *Biochim. Biophys. Acta*, **974**, 289–293.

Horton, P., Ruban, A.V. and Walters, R.G. (1996) Regulation of light harvesting in green plants. *Annu. Rev. Plant Physiol. Plant Mol. Biol.* **47**, 655–684.

Igarashi, D., Miwa, T., Seki, M., Kobayashi, M., Kato, T., Tabata, S., Shinizaki, K. and Ohsumi, C. (2003) Identification of photorespiratory glutamate: glyoxylate aminotransferase (GGAT) gene in Arabidopsis. *Plant J.* **33**, 975–987.

Igarashi, D., Tsuchida, H., Miyao, M. and Ohsumi, C. (2006) Glutamate:glyoxylate aminotransferase modulates amino acid content during photorespiration. *Plant Physiol.* **142**, 901–910.

Izumi, M., Tsunoda, H., Suzuki, Y., Makino, A. and Ishida, H. (2012) RBCS1A and RBCS3B, two major members within the Arabidopsis RBCS multigene family, function to yield sufficient RuBisCO content for leaf photosynthetic capacity. *J. Exp. Bot.* **63**, 2159–2170.

Joshi, V., Laubengayer, K.M., Schauer, N., Fernie, A.R. and Jander, G. (2006) Two Arabidopsis threonine aldolases are nonredundant and compete with threonine deaminase for a common substrate pool. *Plant Cell.* **18**, 3564–3575.

Kebeish, R., Niessen, M., Thiruveedhi, K., Bari, R., Hirsh, H.-J., Rosenkranz, R., Stäbler, N., Schönfeld, B., Kreuzaler, F. and Peterhänsel, C. (2007) Chloroplastic photorespiratory bypass increases photosynthesis and biomass production in *Arabidopsis thaliana*. *Nature Biotech.* **25**, 593–599.

Laemmli, U.K. (1970) Cleavage of structural proteins during the assembly of the head of bacteriophage T4. *Nature*, **227**, 680–685.

Laisk, A. and Sumberg, A. (1994) Partitioning of the leaf CO_2 exchange into components using CO_2 exchange and fluorescence measurements. *Plant Physiol.* **106**, 689–695.

Liepman, A.H. and Olsen, L.J. (2003) Alanine aminotransferase homologs catalyze the glutamate:glyoxylate aminotransferase reaction in peroxisomes of Arabidopsis. *Plant Physiol.* **131**, 215–227.

Lu, Y., Li, Y., Yang, Q., Zhang, Z., Chen, Y., Zhang, S. and Peng, X.-X. (2013) Suppression of glycolate oxidase causes glyoxylate accumulation that inhibits photosynthesis through deactivating RuBisCO in rice. *Physiol. Plant.* **150**, 463–476.

Maier, A., Fahnenstich, H., von Caemmerer, S., Engqvist, M.K.M., Weber, A.P.M., Flügge, U.-I. and Maurino, V.G. (2012) Transgenic introduction of a glycolate oxidative cycle into *A. thaliana* chloroplasts leads to growth improvement. *Front. Plant Sci.* **3**, 1–12.

Maxwell, K. and Johnson, G.N. (2000) Chlorophyll fluorescence-a practical guide. *J. Exp. Bot.*, **51**, 659–668.

Mulligan, R.M., Wilson, B. and Tolbert, N.E. (1983) Effects of glyoxylate on photosynthesis by intact chloroplasts. *Plant Physiol.* **72**, 415–419.

Noctor, G., Bergot, G., Mauve, C., Thominet, D., Lelarge-Trouverie, C. and Prioul, J.-L. (2007) A comparative study of amino acid measurements in leaf extracts by gas chromatography-time of flight-mass spectrometry and high performance liquid chromatography with fluorescence detection. *Metabolomics*, **3**, 161–174.

Nölke, G., Houdelet, M., Kreuzaler, F., Peterhänsel, C. and Schillberg, S. (2014) The expression of a recombinant glycolate dehydrogenase polyprotein in potato (*Solanum tuberosum*) plastids strongly enhances photosynthesis and tuber yield. *Plant Biotech. J.* **6**, 734–742.

Peterson, R.B. and Havir, E.A. (2001) Photosynthetic properties of an *Arabidopsis thaliana* mutant possessing a defective PsbS gene. *Planta*, **214**, 142–152.

Porra, R.J., Thompson, W.A. and Kriedmann, P.E. (1989) Determination of accurate extinction coefficients and simultaneous equations for assaying chlorophylls *a* and *b* extracted with four different solvents: verification of the concentration of chlorophyll standards by atomic absorption spectroscopy. *Biochim. Biophys. Acta*, **975**, 384–394.

Queval, G. and Noctor, G. (2007) A plate reader method for the measurement of NAD^+, $NADP^+$, glutathione, and ascorbate in tissue extracts: Application to redox profiling during Arabidopsis rosette development. *Anal. Biochem.* **363**, 58–69.

Quick, W.P., Schurr, U., Fichtner, K., Schulze, E.-D., Rodermel, S.R., Bogorad, L. and Stitt, M. (1991) The impact of decreased RuBisCO on photosynthesis, growth, allocation and storage in tobacco plants which have been transformed with antisense *rbcS*. *Plant J.* **1**, 51–58.

Rachmilevitch, S., Cousins, A.B. and Bloom, A.J. (2004) Nitrate assimilation in plant shoots depends on photorespiration. *Proc. Natl Acad. Sci. USA*, **101**, 11506–11510.

Rojas, C.M., Senthil-Kumar, M., Wang, K., Ryu, C.M., Kaudal, A. and Mysore, K.S. (2012) Glycolate oxidase modulates reactive oxygen species-mediated signal transduction during nonhost resistance in Nicotiana benthamiana and Arabidopsis. *Plant Cell.* **24**, 336–352.

Ros, R., Muñoz-Bertomeu, J. and Krueger, S. (2014) Serine in plants: biosynthesis, metabolism, and functions. *Trends Plant Sci.*, **19**, 564–569.

Rott, M., Martins, N.F., Thiele, W., Lein, W., Bock, R., Kramer, D.M. and Schöttler, M.A. (2011) ATP synthase repression in tobacco restricts photosynthetic electron transport, CO_2 assimilation, and plant growth by over acidification of the thylakoid lumen. *Plant Cell.*, **23**, 304–321.

Somerville, C.R. and Ogren, W.L. (1980) Photorespiration mutants of *Arabidopsis thaliana* deficient in serine-glyoxylate aminotransferase activity. *Proc Nat. Acad. Sci. USA*, **77**, 2684–2687.

Somerville, C.R. and Ogren, W.L. (1981) Photorespiration-deficient mutants of *Arabidopsis thaliana* lacking mitochondrial serine transhydroxymethylase activity. *Plant Physiol.*, **67**, 666–671.

Somerville, C.R. and Ogren, W.L. (1982) Mutants of the cruciferous plant *Arabidopsis thaliana* lacking glycine decarboxylase activity. *Biochem. J.*, **202**, 373–380.

Sudo, E., Suzuki, Y. and Makino, A. (2014) Whole-plant growth and N utilization in transgenic rice plants with increased or decreased RuBisCO content under different CO_2 partial pressures. *Plant Cell Physiol.*, **55**, 1905–1911.

Takahashi, S., Bauwe, H. and Badger, M. (2007) Impairment of the photorespiratory pathway accelerates photoinhibition of photosystem II by suppression of repair but not acceleration of damage processes in Arabidopsis. *Plant Physiol.*, **144**, 487–494.

Tcherkez, G., Bligny, R., Gout, E., Mahé, A., Hodges, M. and Cornic, G. (2008) Respiratory metabolism of illuminated leaves depends on CO_2 and O_2 conditions. *Proc. Natl Acad. Sci. USA*, **105**, 797–802.

Timm, S. and Bauwe, H. (2013) The variety of photorespiratory phenotypes–employing the current status for future research directions on photorespiration. *Plant Biol.*, **15**, 737–747.

Timm, S., Mielewszik, M., Florian, A., Frankenbach, S., Dreissen, A., Hocken, N., Fernie, A.S., Walter, A. and Bauwe, H. (2012) High-to-low CO_2 acclimation reveals plasticity of the photorespiratory pathway and indicates regulatory links to cellular metabolism of Arabidopsis. *PLoS ONE*, **7**, e42809.

Ward, D.A. and Keys, A.J. (1989) A comparison between the coupled spectrophotometric and uncoupled radiometric assays for RuBP carboxylase. *Photosynth. Res.*, **22**, 167–171.

Xu, H., Zhang, J., Zeng, J., Jiang, L., Liu, E., Peng, C., He, Z. and Peng, X. (2009) Inducible antisense suppression of glycolate oxidase reveals its strong regulation over photosynthesis in rice. *J. Exp. Bot.*, **60**, 1799–1809.